AD NUMBER
AD079806
LIMITATION CHANGES

TO:

Approved for public release; distribution is unlimited. Document partially illegible.

FROM:

Distribution authorized to U.S. Gov't. agencies and their contractors; Administrative/Operational Use; 21 SEP 1953. Other requests shall be referred to Naval Ordnance Laboratory, White Oak, MD. Document partially illegible.

AUTHORITY
USNOL ltr, 29 aug 1974

AD 79806

Armed Services Technical Information Agency

Reproduced by

DOCUMENT SERVICE CENTER
KNOTT BUILDING, DAYTON, 2, OHIO

UNCLASSIFIED

FC

NOL WIND-TUNNEL INTERNAL STRAIN-GAGE BALANCE SYSTEM

21 SEPTEMBER 1953

U. S. NAVAL ORDNANCE LABORATORY

WHITE OAK, MARYLAND

NOL WIND-TUNNEL INTERNAL STRAIN-GAGE BALANCE SYSTEM

Prepared by:

I. Shantz
B. D. Gilbert
C. E. White

ABSTRACT: This report describes some of the general design features, both electrical and mechanical, currently used in the construction of internal strain-gage balances. Among the design features discussed are the geometric shape of the individual measuring sections, the placement and bonding of the strain gages to these sections, and the wiring circuits used. A large portion of this report is devoted to the methods of calibration and derivations of the data reduction equations which convert raw data into aerodynamic coefficients. This work was carried out under NOL Task M9a-133-1-54.

This report is one of a series of three which have been prepared for use by personnel or organizations who will be using the facilities of the Naval Ordnance Laboratory for developmental wind-tunnel testing work. This report describes the design and use of internal strain-gage balances to obtain aerodynamic design data.

The system used for recording wind-tunnel force, moment, and pressure data as received from electrical resistance strain-gage balances is described in reference (a).

Reference (b) contains a general description of the wind-tunnel plant and facilities, testing procedures, and general administrative information.

The authors wish to acknowledge the efforts of the many Naval Ordnance Laboratory personnel whose work has been included in this report and particularly the original work of Dr. G. L. Shue in the development of the internal strain-gage balances.

JOHN T. HAYWARD
Captain, USN
Commander

N. H. KURZWEG, Chief
Aeroballistic Research Department
By direction

Contents

Illustrations

NOL WIND-TUNNEL INTERNAL STRAIN-GAGE BALANCE SYSTEM

INTRODUCTION

1. The purpose of this report is to acquaint the reader with the internal strain-gage balance techniques and attendant equipment as they are currently used for wind-tunnel investigations performed in the NOL 40 x 40 cm Aeroballistics Tunnels.

2. Internal strain-gage balances have been in use in the wind tunnels at the Naval Ordnance Laboratory for some time. Internal strain-gage balances have a number of very definite advantages, as compared to external mechanical balances, in that they are compact, more sensitive, give stabilized readings much more rapidly, and do not require tare readings. This is particularly desirable in an intermittent installation such as is in use at the Naval Ordnance Laboratory.

3. Electric resistance strain gages consist of grids of resistance wire imbedded in thin sheets of bakelite which can be cemented to structural members. Under strain, the resistance grid distorts with the member and changes resistance proportionally to the elongation or contraction of the member. The strain-gages used on the Naval Ordnance Laboratory balances are Baldwin-Lima-Hamilton, type SR-4, generally of 120 ohms resistance. Each of the load components is measured by four strain-gages wired in a Wheatstone Bridge arrangement.

Symbols

Free-Stream Flow Parameters

M = Mach number

q = impact pressure (psi) = $1/2 \rho v^2 \times 1/144$

ρ = density of stream (slugs/ft^3)

v = free-stream velocity (ft/sec)

Force and Moments

(1) Forces

D = drag force (pounds) (wind axes)

F = axial force (pounds) (balance axes)

L = lift force (pounds) (wind axes)

N = normal force (pounds) (balance axes)

Y = lateral or yaw force (pounds) (balance axes)

1

Symbols (continued)

(2) <u>Moments</u>

M_ϕ = rolling moment (inch-pounds)

M_ψ = yawing moment (inch-pounds)

M_θ = pitching moment (inch-pounds)

(3) <u>Reference points</u> (stations along balance axis)

$X_{c.g.}$ = $\overline{X}$ = center of gravity location (reference for pitching and yawing moments)

$X_{c.p.}$ = center of pressure location

X_c = electrical center of gage

X_1 = electrical center of forward pitching moment gage

X_2 = electrical center of aft pitching moment gage

X_3 = electrical center of forward yawing moment gage

X_4 = electrical center of aft yawing moment gage

X_7 = electrical center of axial force gage acting as a pitching moment gage (interaction)

X_8 = electrical center of axial force gage acting as a yawing moment gage (interaction)

<u>Angular Orientation</u>

α = angle of attack (degrees) (pitch plane)

ϕ = angle of roll (degrees) (angular displacement in plane transverse to balance axis)

ψ = angle of yaw (degrees) (yaw plane)

<u>Reference Dimensions</u>

(1) <u>Missile</u>

A = cross-sectional area (inch^2)

d = nominal body diameter (inches)

Symbols (continued)

(2) <u>Aircraft</u>

  b = wing span (inches)

  c = wing mean aerodynamic chord (inches)

  s = wing area (inches)^2

Aerodynamic Coefficients

  C_A = axial force coefficient = $F/q.S$

  C_D = drag force coefficient = $D/q.S$

  C_L = lift force coefficient = $L/q.S$

  C_N = normal force coefficient = $N/q.S$

  C_Y = yaw force coefficient = $Y/q.S$

  C_ϕ = rolling moment coefficient = $M_\phi/q.S.d$

  C_ψ = yawing moment coefficient = $M_\psi/q.S.d$

  C_θ = pitching moment coefficient = $M_\theta/q.S.d$

Operating Principle of the Internal Strain-Gage Balance

4. The principle of the internal strain-gage balance is a relatively simple one. It is merely a cantilever beam with specially designed cross-sections which are more sensitive (deflect much more) to one type of loading than to any other loading. The ideal condition is a flexure section which will deflect only for the loading to be measured. In practice, it is almost impossible to design and build a balance which is totally free of interaction. Procedures and methods for dealing with these interactions are presented in succeeding paragraphs. Each of the load sensing flexures converts the physical stress it picks up into an electrical signal by means of strain gages which are bonded to the metal at that location.

5. The change in resistance due to deflection of a strain gage is very small. The resultant percentage change in voltage across the gage would, therefore, likewise be very small, and difficult to measure. However, by the use of bridge circuits, it is possible to balance out the initial voltage, and to have the small change produced indicate as an absolute change which can then be measured with moderately sensitive instruments. The other three arms of the bridge could be fixed resistances, but by arranging other strain gages to be used as the

other arms of the bridge, it is possible to obtain four times the
voltage change. Furthermore, since all gages are located close together
and all are subjected to the same temperature changes, any such changes
affecting the resistance of one gage would theoretically affect all of
the gages equally, thus eliminating temperature effect from the indication
of the balance. Also, as indicated elsewhere in this report, effects of
forces or moments other than the one to be measured may likewise be
minimized through the use of the four arm balance. Thus most of the
balances used at the Naval Ordnance Laboratory Aeroballistic Research
Facility use the four arm arrangement. Typical arrangements of balances
are described in the following paragraphs.

Pitching Moment and Yawing Moment Sections

6. Shown in Figure 1 is a typical section which will measure both
pitching moment and yawing moment simultaneously. The dimensions of the
cross-section of the pitch or yaw component are determined by the
magnitude of the normal or yaw force expected and by the location of the
centers of pressure. The moments exerted at this section are a function
of both force and point of application; therefore, it is possible to use
the same cross-sectional dimensions for a variety of aerodynamic loadings,
within allowable stress tolerances. The upper limit of allowable strain
is determined by the strain gage. The manufacturer's recommendation is
four to five thousand micro-inches per inch, which is roughly equivalent
to a stress of 120,000 to 150,000 psi for steel; however, this upper limit
is seldom approached for static loads. The lower limit is determined by
the amplifier characteristics of the electronic strain indicator equipment.
From experience, employing the strain indicator equipment now available at
the Naval Ordnance Laboratory for this work, a stress of 100 psi has been
successfully measured. These stress and strain considerations are general
and apply to all of the components measured by the balance.

7. A pitch force, P, applied to the balance as shown in Figure 2A,
will subject this section to a bending moment. If these gages are
connected electrically as shown in Figure 2B, with a potential v applied
across points J and K no voltage difference will appear across points A
and B if all of the resistances are equal in value. With a bending moment
exerted at this section gages 1 and 3 have increased in resistance and
gages 2 and 4 have decreased in resistance; thus, point A is at a lower
potential than it was with no bending and point B is at a higher potential.
It is the potential difference between these two points that provides the
means for quantitatively determining the moment.

Rolling Moment Balance Section

8. There are a number of various sections that will measure rolling
moment; however, the cruciform section as shown in Figure 3A is most
commonly used at the Naval Ordnance Laboratory. Its major advantages
are compactness, ease of manufacture, and simplicity in mounting and
wiring of the individual strain gages. The roll section of the balance
is generally located, when practicable, near the expected centers of
pressure of the model. This tends to reduce the effects of pitching
and yawing moment interactions.

9. It is possible to wire this section in such a manner as to minimize interaction effects, see Figure 3B. For example, if a rolling moment (M∅) is applied to the balance, gages 1 and 3 will be in compression (reducing resistance) while gages 2 and 4 will be in tension (increasing resistance). This will create an unbalance in the Wheatstone Bridge circuit and enables this component to be measured. However, a pitch force (P) applied as shown in Figure 3A, will place gages 1 and 2 in tension and gages 3 and 4 in compression, theoretically, causing no potential difference across points A and B. A yaw force (Y) would be cancelled in the same manner since gages 1 and 4 would be in compression and gages 2 and 3 would be in tension.

10. It should be noted in Figure 3 that the strain gages are located at the center of the flat section at 45 degrees to the axis of the balance. This is necessary in order to utilize the maximum of mechanical sensitivity available. The stress concentration under torsion is greatest at these points.

Axial Force Balance Section

11. Numerous designs have been proposed and built to measure the axial force component; however, one particular design which has been used most successfully at the Naval Ordnance Laboratory is shown in the diagrammatic sketch in Figure 4A. To date, this design has yielded the most satisfactory results. The interaction on axial force due to pitch and yaw loading are reduced by the mechanical design of this structure. The details of this design are complex and not within the scope of this report. However, the important considerations used in the strain-gage placement and circuitry will in general hold true for other axial force balances.

12. Wiring gages 1, 2, 3, and 4 in the manner shown in Figure 4B, would permit the axial force (F) to be measured. Gages 1 and 3 are in tension and gages 2 and 4 in compression when the balance is subjected to an axial load. Due to the rapid change of temperature in the intermittent supersonic wind tunnels, a temperature effect will be in evidence. This is mainly due to Section B not cooling and contracting at the same rate as the outer structure of the balance. The gage section would, therefore, be stressed in a similar manner as if an axial force were acting.

13. In order to compensate for this temperature effect four more gages are placed on the after web as shown in Figure 4A. Wiring these gages into an individual bridge and placing this bridge in parallel, as shown in Figure 4C, will eliminate the temperature effect. An axial force applied to the same structure will now cause gages 1, 3, 5, and 7 to be in tension and gages 2, 4, 6, and 8 to be in compression, thus creating an unbalance in both bridges which are mutually aiding. A change in temperature, as described in the preceding paragraph, will cause gages 1, 3, 6, and 8 to be stressed in tension. Each individual bridge is now unbalanced but in opposite directions, thus opposing each other and resulting in a zero unbalance for the circuit as a whole.

5

14. A photograph of a six-component balance used in developmental testing is presented in Figure 5. The axial section in this balance utilizes the parallel two bridge circuit.

Mounting of SR-4 Bakelite Strain Gages

15. The efficiency of a balance depends to a large extent on the proper application of the strain gages. Therefore, great care must be taken in preparing and cementing the strain gages to the flexible members of the balance. A good bond will facilitate balancing of the complete bridge circuit and help to reduce temperature effect to a minimum.

16. Each bridge circuit should contain four matched strain gages. These gages must be equal in resistance to within one tenth of an ohm and contain the same gage factor:

$$\text{Gage factor } G = \frac{\Delta R}{R} \Big/ \frac{\Delta L}{L}$$

where ΔR is the change of the unstrained resistance R produced by an increment in length ΔL on the original length L. In the event not enough matched strain gages are available, the strain gages of two adjacent arms should be matched.

17. Before assembly, the locations of the gages should be laid out carefully, and the gages should be trimmed, if necessary, to permit them to fit the space available. Care should be taken not to damage the grids of the gages. The surfaces on which the gages are to be mounted should be roughened slightly, by scraping with a sharp knife or other tool, and then cleaned thoroughly with benzine, followed by pure grain alcohol, and finally with acetone. The gages also should be cleaned thoroughly. After drying carefully, care should be taken to avoid touching the surfaces, until the cement is applied.

18. In preparing the cement for use an activator is added to it as it comes from the tube until the proper consistency is obtained. This mixture is then applied to the surface of the metal and also to the back of the gage. The gage is then placed on the metal never exerting more than light contact pressure (finger contact is sufficient). The gage is then very lightly clamped in place and baked in an oven at 220°F for a period of two to four hours.

19. After assembly and before wiring, each strain gage should be checked for insulation resistance. Each gage should have no less than 10,000 megohms between the grid leads and ground. After wiring, they should be checked again and the total insulation resistance should be no less than 1,000 megohms to ground.

6

Determination of Bridge Unbalance

20. There are two basic methods in use for indicating the unbalance which appears across the strain-gage bridge. The first method is shown in Figure 6A. In this method, the input terminals of the bridge (J and K) are shunted by the end connections of a potentiometer type variable resistance. The slider is connected to one of the other terminals through a calibration resistance (R_c). When the bridge is unbalanced, by application of a load to the balance, the output voltage can be reduced to zero by moving the slider on the potentiometer. The amount of motion required is dependent on the size of the load and the value of the calibration resistance (R_c). The null condition can be determined to within one microvolt by using an amplifier shunted across the output terminals. The amplifier can be connected to an indicating meter to show a null. More usually however, it is connected to a servo motor which automatically drives the slider of the potentiometer to a null point.

21. The second method is shown in Figure 6B. In this system the voltage unbalance is "bucked out" by an equal and opposite voltage to obtain a null reading. The amount of variation of the slider position is dependent on the value of R_c in series with the "bucking" voltage supply. In the first system, the reading of the slider dial is independent of the voltage applied to the bridge. This is also true of the second system if the bridge and "bucking" voltages are equal or vary proportionally. The first system is unaffected in calibration by any filters applied across the bridge output or amplifier terminals. However, these filters may give rise to servo problems since they become part of the regulatory loop. In the second system, the impedance of the filters may conceivably load the bridge and change the calibration, but they would not be part of the regulatory loop.

22. Manual data recording is generally taken with a 400 cycle bridge supply, servo controlled recording is taken with 60 cycle bridge supply. The servo driven balance detection system is adaptable to automatic recording of data on punched cards. This system is generally used at the Naval Ordnance Laboratory wind tunnels to improve accuracy of transcription. A photograph of this equipment is shown in Figure 7. Details of the procedures used for calibration, taking of data, and computation techniques are described in the next section of this report.

Calibration Procedures and Data Reduction Equations

23. Calibration of an internal strain-gage balance consists mainly of applying to the balance similar loads as would be encountered in the wind-tunnel test. Each component is calibrated separately. In calibration, the weights and loading stations are known and from these the gage constants can be determined.

24. In the succeeding paragraphs the calibration techniques and data reduction equations for each component are grouped together, each section combining the complete procedure for one component. This includes calibration technique, derivation of data reduction equations, and interaction equations if applicable.

7

Calibration of Pitching and Yawing Moments

25. The calibration procedure for pitching moment and yawing moment is exactly the same. The internal strain-gage balances used in the NOL 40 x 40 cm Aeroballistics Tunnels employ the two-moment method for determining normal or side forces. Therefore, it will be sufficient to present the procedure for only one moment gage.

26. The actual calibration procedure can be broken up into three steps in the following manner:

(a) The balance and sting is mounted in a dividing head in the same position that it will occupy in the tunnel, i.e., positive angle of attack up and the balance is leveled.

(b) An arbitrary reference point is chosen on the balance from which the electrical center of the gage can be defined. A very convenient method of doing this is to mount the model body on the balance in the same position as it will be in the tunnel. This directly relates the electrical center of the gage to some arbitrary point on the model, i.e., base of the model.

(c) Calibrated weights are applied to the balance, via model or calibrating body, at defined locations. The change in resistance of the strain gages at the measuring section, due to the applied load, is recorded by the strain indicator equipment for each increment of load applied. The strain indicator equipment yields the change in resistance in units of dial divisions (ΔN) and is related to the actual moment by the equation,

$$M = N (X - X_c) = K (\Delta N)$$

where

M = moment (inch-lbs)

N = normal force, known weights (lbs)

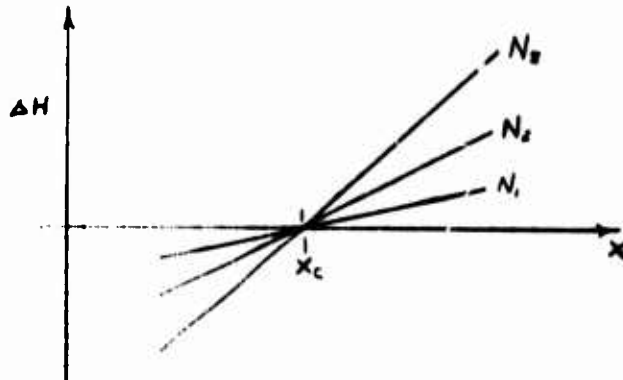K = gage constant (inch-lbs/dial division)

X_c = electrical center of gage (in.)

X = point of application of load (inch)

ΔN = dial divisions of deflection

27. With the known weights hung at a known distance from the reference point, the factor K may be determined. Below is shown a plot of the ΔN values recorded when known weights are hung at various stations along the X axis (body axis).

The point along the axis where the strain is zero, is the electrical center of the gage. The electrical center and the geometric center of the gages may not coincide. This may be due to the manner in which the gages are mounted or it may be a mechanical characteristic of the balance, or a combination of both. The same procedures apply for yawing moment loads that apply for pitching moment loads. The only difference being that the balance is rotated 90 degrees counter-clockwise (looking forward from base of model).

Determination of Calibration Constants

(Pitch and Yaw)

$$M = N(x - x_c) = K(\Delta H) \qquad \begin{array}{l} X = \text{loading station} \\ X_c = \text{elec. center} \end{array}$$

$$\frac{K}{N}(\Delta H) = x - x_c$$

$$X - \frac{K}{N}(\Delta H) = x_c$$

$$\frac{X}{X_c} - \frac{K}{X_c}\left(\frac{\Delta H}{N}\right) = 1$$

let

$$Y = \frac{\Delta H}{N} \;;\; \frac{1}{X_c}(x) - \frac{K}{X_c}(Y) = 1 \tag{1}$$

9

Multiply equation (1) by X and by Y to obtain a pair of simultaneous
equations: we have:

$$\left(\frac{1}{X_c}\right) X^2 - \left(\frac{K}{X_c}\right) XY = X \tag{2}$$

$$\left(\frac{1}{X_c}\right) XY - \left(\frac{K}{X_c}\right) Y^2 = Y \tag{3}$$

Taking summations:

$$\left(\frac{1}{X_c}\right) \Sigma X^2 - \left(\frac{K}{X_c}\right) \Sigma XY = \Sigma X \tag{4}$$

$$\left(\frac{1}{X_c}\right) \Sigma XY - \left(\frac{K}{X_c}\right) \Sigma Y^2 = \Sigma Y \tag{5}$$

by determinants:

$$\frac{1}{X_c} = \frac{\begin{vmatrix} \Sigma X & -\Sigma XY \\ \Sigma Y & -\Sigma Y^2 \end{vmatrix}}{\begin{vmatrix} \Sigma X^2 & -\Sigma XY \\ \Sigma XY & -\Sigma Y^2 \end{vmatrix}} = \frac{-\Sigma X \cdot \Sigma Y^2 + \Sigma Y \cdot \Sigma XY}{-\Sigma X^2 \cdot \Sigma Y^2 + (\Sigma XY)^2}$$

$$\frac{K}{X_c} = \frac{\begin{vmatrix} \Sigma X^2 & \Sigma X \\ \Sigma XY & \Sigma Y \end{vmatrix}}{\begin{vmatrix} \Sigma X^2 & -\Sigma XY \\ \Sigma XY & -\Sigma Y^2 \end{vmatrix}} = \frac{\Sigma X^2 \cdot \Sigma Y - \Sigma X \cdot \Sigma XY}{-\Sigma X^2 \cdot \Sigma Y^2 + (\Sigma XY)^2}$$

$$K = \frac{K}{X_c}\left(\frac{1}{\frac{1}{X_c}}\right) = \left[\frac{\Sigma X^2 \cdot \Sigma Y - \Sigma X \cdot \Sigma XY}{-\Sigma X^2 \cdot \Sigma Y^2 + (\Sigma XY)^2}\right]\left[\frac{-\Sigma X^2 \Sigma Y^2 + (\Sigma XY)^2}{-\Sigma X \cdot \Sigma Y^2 + \Sigma Y \cdot \Sigma XY}\right]$$

therefore,

$$K = \frac{\Sigma X^2 \cdot \Sigma Y - \Sigma X \cdot \Sigma XY}{-\Sigma X \cdot \Sigma Y^2 + \Sigma Y \cdot \Sigma XY} \tag{6}$$

$$X_c = \frac{(\Sigma XY)^2 - \Sigma X^2 \cdot \Sigma Y^2}{\Sigma Y \cdot \Sigma XY - \Sigma X \cdot \Sigma Y^2} \tag{7}$$

Derivation of Normal Force and Pitching Moment Reduction Equations

Two Moment Method:
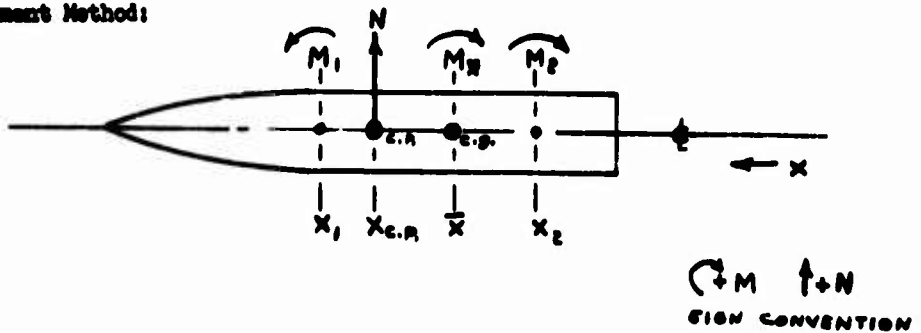
The moments measured at stations X_1 and X_2 are caused by a normal force (N) acting at station $X_{c.p.}$

$$-M_1 = N(X_1 - X_{c.p.}) \tag{8}$$

$$M_2 = N(X_{c.p.} - X_2) \tag{9}$$

$$M_{\bar{x}} = N(X_{c.p.} - \bar{x})$$

$$M_{\bar{x}} = N(X_1 - \bar{x}) + M_1 = M_2 - N(\bar{x} - X_2) \tag{10}$$

adding equations (8) and (9) we have

$$M_2 - M_1 = N\left[X_{c.p.} - X_2 + X_1 - X_{c.n.}\right] = N(X_1 - X_2)$$

solving for N

$$N = \frac{M_2 - M_1}{X_1 - X_2} \qquad (11)$$

Expressing M_2 and M_1 in the form

$$M_1 = K_1(\Delta H)_1 \qquad (12)$$

$$M_2 = K_2(\Delta H)_2 \qquad (13)$$

and substituting into equation (11)

$$N = \frac{K_2(\Delta H)_2}{X_1 - X_2} - \frac{K_1(\Delta H)_1}{X_1 - X_2} \qquad (14)$$

in coefficient form

$$C_N = \frac{K_2(\Delta H)_2}{q \cdot S(X_1 - X_2)} - \frac{K_1(\Delta H)_1}{q \cdot S(X_1 - X_2)} \qquad (15)$$

Solving for the pitching moment at the center of gravity ($M_{\bar{x}}$), substituting equation (11) into (10).

$$M_{\bar{x}} = M_2 - \left[\frac{M_2 - M_1}{X_1 - X_2}\right] \cdot (\bar{X} - X_2)$$

$$M_{\bar{x}} = M_2 - M_2\left[\frac{\bar{X} - X_2}{X_1 - X_2}\right] + M_1\left[\frac{\bar{X} - X_2}{X_1 - X_2}\right]$$

$$M_{\bar{x}} = M_2\left[\frac{X_1 - X_2 + X_2 - \bar{X}}{X_1 - X_2}\right] + M_1\left[\frac{\bar{X} - X_2}{X_1 - X_2}\right]$$

$$M_{\bar{x}} = M_2\left[\frac{X_1 - \bar{X}}{X_1 - X_2}\right] + M_1\left[\frac{\bar{X} - X_2}{X_1 - X_2}\right] \tag{16}$$

using equations (12) and (13)

$$M_{\bar{x}} = K_2(\Delta H)_2\left[\frac{X_1 - \bar{X}}{X_1 - X_2}\right] + K_1(\Delta H)_1\left[\frac{\bar{X} - X_2}{X_1 - X_2}\right] \tag{17}$$

expressing $M_{\bar{x}}$ in coefficient form according to

$$M_{\bar{x}} = C_0 \cdot q \cdot S \cdot d$$

we have

$$C_0 = \frac{K_2(\Delta H)_2}{q \cdot S \cdot d}\left[\frac{X_1 - \bar{X}}{X_1 - X_2}\right] + \frac{K_1(\Delta H)_1}{q \cdot S \cdot d}\left[\frac{\bar{X} - X_2}{X_1 - X_2}\right] \tag{18}$$

For ease of handling in IBM reduction, equations (15) and (18) may be expressed in the form

$$C_N = B_N(\Delta H)_2 - A_N(\Delta H)_1 \tag{19}$$

13

$$C_\theta = B_\theta (\Delta H)_2 + A_\theta (\Delta H)_1$$

(20)

where

$$A_N = \frac{K_1}{\overline{q} \cdot S (X_1 - X_2)} \qquad ; \qquad B_N = \frac{K_2}{\overline{q} \cdot S (X_1 - X_2)}$$

$$A_\theta = \frac{K_1}{\overline{q} \cdot S \cdot d} \left[\frac{\overline{X} - X_2}{X_1 - X_2} \right] \qquad ; \qquad B_\theta = \frac{K_2}{\overline{q} \cdot S \cdot d} \left[\frac{X_1 - \overline{X}}{X_1 - X_2} \right]$$

These constants will change only with Mach number and/or a change in sensitivity. A similar derivation may be used to find the force and moment in the yaw plane, this will yield

$$C_Y = B_Y (\Delta H)_4 - A_Y (\Delta H)_3$$

(21)

$$C_\psi = B_\psi (\Delta H)_4 - A_\psi (\Delta H)_3$$

(22)

where

$$A_Y = \frac{K_3}{\overline{q} \cdot S (X_3 - X_4)} \qquad ; \qquad B_Y = \frac{K_4}{\overline{q} \cdot S (X_3 - X_4)}$$

$$A_\psi = \frac{K_3}{\overline{q} \cdot S \cdot d} \left[\frac{\overline{X} - X_4}{X_3 - X_4} \right] \qquad ; \qquad B_\psi = \frac{K_4}{\overline{q} \cdot S \cdot d} \left[\frac{X_3 - \overline{X}}{X_3 - X_4} \right]$$

14

Elimination of Interactions by Electrical Shunting (pitch and yaw)

28. If a load is applied to a model in one of the reference planes and the strain indicators record forces in a second reference plane, angularly displaced 90 degrees, the indicated forces recorded in the second plane are called interactions. An interaction can be calibrated and removed from the data in the reduction; or it can be partially or completely removed by electrical shunting. Interactions of pitch-on-yaw and yaw-on-pitch can always be entirely removed electrically. Interactions are usually caused by an imperfect alignment of the strain gages. The misalignment may be due to the machining of the balance or to the mounting of the strain gages. Pitch and yaw gages can be aligned electrically (90 degrees apart) by first placing the model on the balance and leveling it, and second, placing equal resistances in parallel with two adjacent arms will bring the Wheatstone Bridge into alignment, as shown in Figure 8. The value of the resistance and the position of the shunts are determined experimentally. Since these interactions are eliminated the problem of data reduction is reduced to the simple form described above.

Axial Force Calibration and Reduction

29. In the calibration of an axial force balance, the increments of load are applied along the longitudinal axis of the balance. An axial calibration is performed with the balance mounted vertically and leveled in this position. The increments of load are applied and the strain indicator deflections are recorded. The indicator readings are related to the axial force by the equation:

$$F = K_6 (\Delta H)_6 = C_A \cdot q \cdot S \tag{23}$$

$$C_A = \frac{K_6}{q \cdot S} (\Delta H)_6 \tag{24}$$

where

$$K_6 = \text{pounds/dial division}$$

To determine K_6 from calibration

$$K_6 = \frac{\sum_{i=1}^{n} \left(\frac{F}{\Delta H}\right)_i}{n} \tag{25}$$

where: n = number of increments used.

Derivation of Axial Force Interactions

30. Interactions on axial force arise from the condition of the axial force gage acting as a pitching and/or yawing moment gage in addition to measuring longitudinal force. These interactions, for balances which have the drag link located inside of the model, are of the order of one to three percent. The form of the pitch interactions on axial force is similar to that of the yaw interaction; therefore, an analysis for only pitch interactions is sufficient to illustrate the method. The conditions of combined loading consisting of a normal load and an axial load can be illustrated in the following diagram:
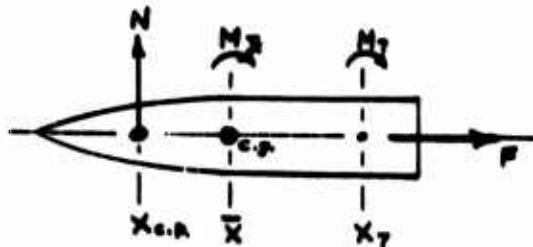
where:
F = axial force (lbs)
N = normal force (lbs)
$X_{c.p.}$ = center of pressure location
$\bar{X}$ = c.g. location
X_7 = elec. center of axial gage acting as a pitch mom. gage

$$M_7 = N\left(X_{c.p.} - X_7\right) = M_{\bar{x}} + N(\bar{X} - X_7) \tag{26}$$

The strain indicator reads the total effect of both axial force and pitch interaction; therefore,

$$\Delta H_T = \Delta H_A + \Delta H_M \tag{27}$$

where:
ΔH_T = total reading
ΔH_A = axial force component
ΔH_M = moment interaction component

Strain indicator readings (ΔH) are related to the component forces and moment by the following equations

$$F = K_6\left(\Delta H_A\right) \tag{28}$$

$$M_7 = K_7\left(\Delta H_M\right) \tag{29}$$

Rearranging equation (27) and substituting in equations (28) and (29).

$$\frac{F}{K_6} = \Delta H_T - \frac{M_7}{K_7} \tag{30}$$

Using the relationship expressed in equation (26), we have

$$\frac{F}{K_6} = \Delta H_T - \frac{M_{\bar{x}}}{K_7} - \frac{N}{K_7}(\bar{x} - x_7) \tag{31}$$

Expressing the forces and moment in coefficient form according to

$$F = C_A \cdot q \cdot S \tag{32}$$

$$M_{\bar{x}} = C_\theta \cdot q \cdot S \cdot d \tag{33}$$

$$N = C_N \cdot q \cdot S \tag{34}$$

we now have

$$\frac{C_A \cdot q \cdot S}{K_6} = \Delta H_T - \frac{C_\theta \cdot q \cdot S \cdot d}{K_7} - \frac{C_N \cdot q \cdot S}{K_7}(\bar{x} - x_7) \tag{35}$$

solving for C_A

$$C_A = \frac{K_6}{q \cdot S}(\Delta H_T) - C_\theta \cdot d\left(\frac{K_6}{K_7}\right) - C_N(\bar{x} - x_7)\frac{K_6}{K_7} \tag{36}$$

Performing a similar analysis for the combined conditions of yaw load and axial load, we have

$$C_A = \frac{K_6}{q \cdot S}(\Delta H_T) - C_\psi \cdot d\left(\frac{K_6}{K_8}\right) - C_Y(\bar{x} - x_8)\frac{K_6}{K_8} \tag{37}$$

For the general combined load condition where pitch, yaw, and axial force loads are applied; equations (36) and (37) are combined and the final reduction equation becomes:

$$C_A = \frac{K_6}{q \cdot S}(\Delta H)_T - C_N(\bar{x} - x_T)\frac{K_6}{K_7} - C_Y(\bar{x} - x_8)\frac{K_6}{K_8} \quad (38)$$

$$- C_\Theta \cdot d\left(\frac{K_6}{K_7}\right) - C_\psi \cdot d\left(\frac{K_6}{K_8}\right)$$

where ΔH_T contains moment components due to pitching and yawing moments.

For simplification and ease in IBM reduction, equation (38) may be written

$$C_A = A_A(\Delta H_T) - S_N \cdot C_N - S_Y \cdot C_Y - S_\Theta \cdot C_\Theta - S_\psi \cdot C_\psi \quad (39)$$

where

$$A_A = \frac{K_6}{q \cdot S}$$

$$S_N = \frac{K_6}{K_7}(\bar{x} - x_T) \qquad ; \qquad S_Y = \frac{K_6}{K_8}(\bar{x} - x_8)$$

$$S_\Theta = d \cdot \frac{K_6}{K_7} \qquad ; \qquad S_\psi = d \cdot \frac{K_6}{K_8}$$

The "S" constants do not change throughout the entire test, i.e., changes in K_6 sensitivity also changes K_7 and K_8 in equal proportion. The constant (A_A) will change with Mach number and sensitivity of the axial force gage.

Rolling Moment Calibration and Reduction

31. In performing a rolling moment calibration, it is necessary to use a special rolling moment rig. This rig consists of a clamp which attaches to the model and has an arm which extends horizontally out and is perpendicular to the model axis. The arm extends out an equal length on each side of the model axis. The arm contains two machined grooves, one at each end. The grooves are equally spaced from the model axis (four inches from the model axis) and are designed to allow a weight pan at each groove. The load necessary to give the proper rolling moment

is split into two sections. One half of the load is placed on each
pan. The channel is then balanced and the load is transferred in
increments from one pan to the other applying positive or clockwise
rolling moment (looking forward from the base). All of the weights
are transferred and then the procedure is reversed and all of the
weights are taken across, still in increments, to the opposite pan;
thus imparting negative rolling moment to the model. After all of the
weights have been transferred to the opposite pan, half of the load
is returned to the original pan, again in increments, and the original
condition of equilibrium is reached. Strain indicator readings are
taken after each increment of load transferred throughout the entire
procedure. A linear relationship exists between the rolling moment
applied and the strain indicator deflection, expressed by the equation

$$M_\phi = W \cdot (\text{MOMENT ARM}) = K_5 (\Delta H)_5 \qquad (40)$$

    W = weight (pounds)

where:

        moment arm = distance from center line of balance to weight
                    pan (inches)

    K_5 = inch-pounds/dial division

To determine K_5 from calibration,

$$K_5 = \frac{\sum_{i=1}^{n} \left(\frac{M_\phi}{\Delta H_5}\right)_i}{n} \qquad (41)$$

where: n = number of increments used

A rolling moment interaction due to the application of a normal or
yaw load can usually be removed electrically, as described in paragraph 28.
However, it is not always possible to entirely remove the interaction by
shunting; it then becomes necessary to calibrate the interaction and
remove its effect in the data reduction. A derivation of the interaction
equations and their application follows:

Derivation of Roll Interaction Equations

    32. Physically it can be said that the balance axis and the roll
axis are skewed lines in space. In evaluating the interaction of a
normal or yaw force on roll, we deal with the projections of the roll
axis on a horizontal plane which passes through the balance axis. The
following diagram illustrates this concept.
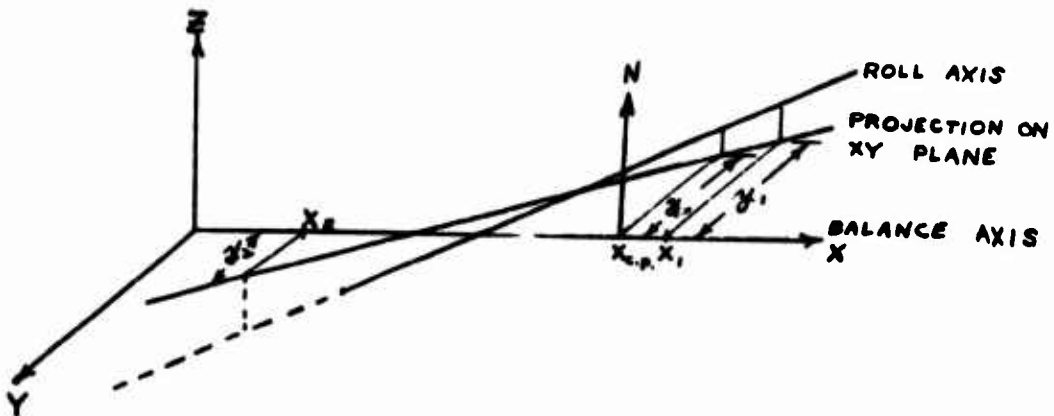
Taking a body cross-section at station X_1 along the balance axis, it would appear as,
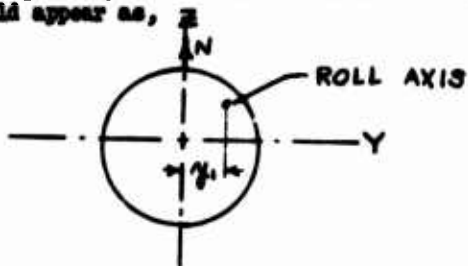
X axis vertical with plane of paper

The rolling moment ($M\phi$) obtained at station X_1 by a normal force applied as shown is

$$M_{\phi_1} = N \cdot \gamma_1 = K_5 (\Delta H_\lambda)_1$$

therefore   (42)

$$\gamma_1 = \frac{K_5 (\Delta H_\lambda)_1}{N}$$

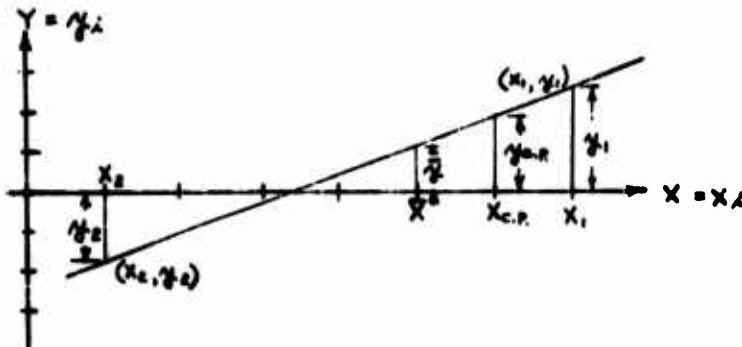The same normal force (N) applied at station X_2 will yield

$$M_{\phi_2} = N \cdot \gamma_2 = K_5 (\Delta H_\lambda)_2$$

and

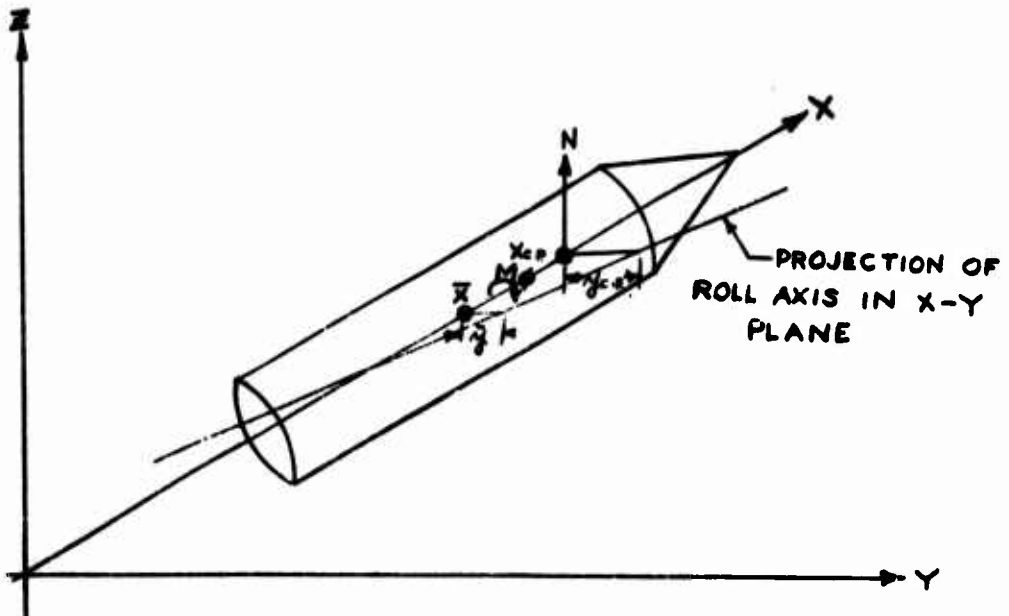$$\gamma_2 = \frac{K_5 (\Delta H_\lambda)_2}{N}$$ (43)

Taking the values of y_1 and y_2, obtained at stations X_1 and X_2 respectively, and plotting them in the X Y plane yields:

This plot will form the basis from which the interaction constants are determined.

The case where there is a rolling moment and a normal force acting on a body can be illustrated by the following diagram.

PROJECTION OF ROLL AXIS IN X-Y PLANE

The total rolling moment read (M_{ϕ_T}) consists of the true rolling moment (M_ϕ) plus an interaction moment (M_{ϕ_i}).

$$M_{\phi_T} = M_\phi + M_{\phi_i}$$

(44)

From the above diagram

$$M_{\phi_i} = N \cdot y_{c.p.}$$

(45)

where

$$y_{c.p.} = \bar{y} + m(x_{c.p.} - \bar{x})$$

(46)

where m = slope of y, X curve = $\dfrac{\Delta y}{\Delta X}$

therefore,

$$M_{\phi_i} = N\left[\bar{y} + m(x_{c.p.} - \bar{x})\right]$$

(47)

from equation (10)

$$M_{\bar{x}} = N(x_{c.p.} - \bar{x})$$

therefore,

$$M_{\phi_i} = N \cdot \bar{y} + m M_{\bar{x}}$$

(48)

defining the quantities in equation (44) by

$$M_{\phi_i} = K_\sigma(\Delta H_i)$$

$$M_\phi = K_\sigma(\Delta H_\sigma)$$

(49)

and stating that the total reading (ΔH_T) in dial division of the rolling moment gage is made up of the true rolling moment component (ΔH_σ) and the interaction component (ΔH_i) yields

$$\Delta H_T = \Delta H_\sigma + \Delta H_i \qquad \text{OR}$$

$$\Delta H_\sigma = \Delta H_T - \Delta H_i$$

(50)

substituting for ΔH, yields

$$\frac{M\phi}{K_S} = \Delta H_T - \frac{M\phi_i}{K_\sigma} = \Delta H_T - \frac{(N \cdot \bar{y} + m \cdot M_{\bar{x}})}{K_S}$$

$$M\phi = K_S(\Delta H_I) - N \cdot \bar{y} - m \cdot M_{\bar{x}} \tag{51}$$

In coefficient form, we have

$$C_\phi \cdot q \cdot S \cdot d = K_S(\Delta H_T) - C_N \cdot q \cdot S \cdot \bar{y} - m \cdot C_\Theta \cdot q \cdot S \cdot d$$

$$C_\phi = \frac{K_S(\Delta H_T)}{q \cdot S \cdot d} - C_N\left(\frac{\bar{y}}{d}\right) - m \cdot C_\Theta \tag{52}$$

For the case where a rolling moment and a yaw force are applied, the reduction equation would be,

$$C_\phi = \frac{K_S(\Delta H_T)}{q \cdot S \cdot d} - C_Y\left(\frac{\bar{z}}{d}\right) - n \cdot C_\psi \tag{53}$$

where $\bar{z}$ and n are the equivalent of $\bar{y}$ and m respectively, but acting in the X Z plane. For the most general case where normal force, yaw force, and rolling moment are all present, the complete reduction equation is

$$C_\phi = \frac{K_S(\Delta H_T)}{q \cdot S \cdot d} - C_N\left(\frac{\bar{y}}{d}\right) - C_Y\left(\frac{\bar{z}}{d}\right)$$

$$- m C_\Theta - n C_\psi \tag{54}$$

more simply stated

$$C_\phi = A\phi(\Delta H_T) - T_N \cdot C_N - T_Y \cdot C_Y - T_\Theta \cdot C_\Theta - T_\psi \cdot C_\psi \tag{55}$$

where $A\phi = \dfrac{K_S}{q \cdot S \cdot d}$; $T_N = \dfrac{\bar{y}}{d}$; $T_Y = \dfrac{\bar{z}}{d}$;

$$T_\Theta = m \quad ; \quad T_\psi = n$$

Static Angle Correction for Balance Deflection

33. An internal strain-gage balance measures the loads acting by
the deflections the loads impose on it. These deflections introduce an
increment to the angle of attack of the model which must be taken into
account in the final reduction of the data. Calibration data to apply
a $\Delta\alpha$ correction is obtained by loading the model in a fashion similar
to a pitch or yaw load calibration. Known weights are applied at defined
stations along the balance axis. The static deflection of the balance
due to each increment of load is measured optically. With this data,
it is possible to compute the change in angle of attack due to the
deflection of the balance under load. The following diagram illustrates
the geometry of the optical apparatus used.
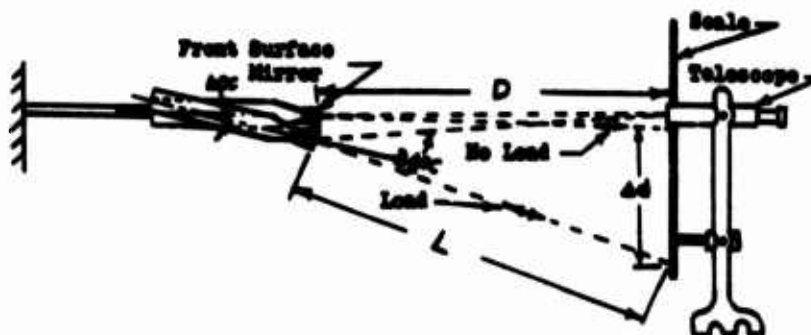
For small angles of $\Delta\alpha$, $D = L$ and Δd approximates the length of the
arc subtended by $2\Delta\alpha$. Therefore,

$$\Delta\alpha = \frac{\Delta d}{2D} (57.3) \quad \text{(degrees)} \tag{56}$$

In order for the above simplifying assumptions to be valid, the distance D
must be at least ten feet. This will also increase the reading accuracy
on the scale.

A plot of $\Delta\alpha/N$ versus station location (X) will yield a linear
relationship
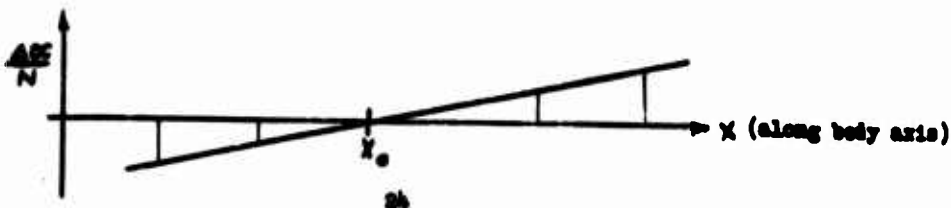
Letting $y = \frac{\Delta \alpha}{N}$ and applying a method of least squares fit to solve for the slope (J) of the curve above and the center of bending (X_0), we have

$$X_0 = \frac{\Sigma x \cdot \Sigma y^2 - \Sigma y \cdot \Sigma x y}{n \cdot \Sigma y^2 - (\Sigma y)^2} \tag{57}$$

$$J = \frac{n \cdot \Sigma y^2 - (\Sigma y)^2}{n \cdot \Sigma x y - \Sigma y \cdot \Sigma x} \tag{58}$$

n = number of terms in array

J = conversion constant (degrees/in-lb)

The equation for $\Delta \alpha$ can now be written as

$$\Delta \alpha = J \cdot N(X - X_0) \tag{59}$$

To facilitate direct reduction by IBM, equation (59) is modified in the following manner

$$\Delta \alpha = J \cdot N\left(X - \overline{X} - X_0 + \overline{X}\right)$$

$$\Delta \alpha = J \cdot N\left(X - \overline{X}\right) - J \cdot N\left(X_0 - \overline{X}\right) \tag{60}$$

let $X = X_{c.p.}$ and using the relationship expressed in equation (10) and rewriting in coefficient form, yields

$$\Delta \alpha = J \cdot C_\theta \cdot q \cdot S \cdot d - J \cdot C_N \cdot q \cdot S\left(X_0 - \overline{X}\right) \tag{61}$$

Employing the following relationships (derived in the data reduction, two moment method)

$$C_\theta = \frac{K_2(\Delta H_2)}{q \cdot S \cdot d}\left[\frac{X_1 - \overline{X}}{X_1 - X_2}\right] + \frac{K_1(\Delta H_1)}{q \cdot S \cdot d}\left[\frac{\overline{X} - X_2}{X_1 - X_2}\right] \tag{62}$$

$$C_N = \frac{K_2(\Delta H_2)}{q \cdot S(X_1 - X_2)} - \frac{K_1(\Delta H_1)}{q \cdot S(X_1 - X_2)} \tag{63}$$

25

equation (61) now becomes:

$$\Delta \alpha = J \cdot K_2 (\Delta H_2) \left[\frac{X_1 - X_0}{X_1 - X_2} \right] + J \cdot K_1 (\Delta H_1) \left[\frac{X_0 - X_2}{X_1 - X_2} \right] \tag{64}$$

Defining α as the angle of attack in the pitch plane and ψ as the angle of attack in the yaw plane (angle of yaw); equation (64) as used in the data reduction, now becomes

$$\alpha = \alpha_{INDICATED} + \Delta \alpha$$

$$\alpha = \alpha_{INDICATED} + J_\theta \cdot K_2 (\Delta H_2) \left[\frac{X_1 - X_0^\theta}{X_1 - X_2} \right] + J_\theta \cdot K_1 (\Delta H_1) \left[\frac{X_0^\theta - X_2}{X_1 - X_2} \right] \tag{65}$$

$$\psi = \psi_{INDICATED} + \Delta \psi$$

$$\psi = \psi_{INDICATED} + J_\psi \cdot K_4 (\Delta H_4) \left[\frac{X_3 - X_0^\psi}{X_3 - X_4} \right] + J_\psi \cdot K_3 (\Delta H_3) \left[\frac{X_0^\psi - X_4}{X_3 - X_4} \right] \tag{66}$$

Equations (65) and (66) may be more simply stated in the following form,

$$\alpha = \alpha_{INDICATED} + E_\alpha (\Delta H_2) + D_\alpha (\Delta H_1)$$

$$\tag{67}$$

$$\psi = \psi_{INDICATED} + E_\psi (\Delta H_4) + D_\psi (\Delta H_3)$$

$$\tag{68}$$

where:

$$E_\alpha = J_\theta \cdot K_2 \left[\frac{X_1 - X_0^\theta}{X_1 - X_2} \right] \qquad ; \quad D_\alpha = J_\theta \cdot K_1 \left[\frac{X_0^\theta - X_2}{X_1 - X_2} \right]$$

$$E_\psi = J_\psi \cdot K_4 \left[\frac{X_3 - X_0^\psi}{X_3 - X_4} \right] \qquad ; \quad D_\psi = J_\psi \cdot K_3 \left[\frac{X_0^\psi - X_4}{X_3 - X_4} \right]$$

note: X_0^θ may not be the same as X_0^ψ as a result of the geometry of the balance.

subscripts or superscripts

θ - denote pitch plane
ψ - denote yaw plane

34. The preceding paragraphs have described in detail techniques involved in the use of the internal strain-gage balance system to measure static forces and moments in the NOL wind tunnels. The balance sections mentioned herein were designed to utilize strain gages as the sensing elements. A number of new designs for internal balances have been proposed and some of these are now in the development stage. One of the designs being developed at the present time is an extremely small internal axial balance to be used primarily in small low-drag models. High sensitivity is achieved by using a linear differential transformer (Schaevitz Coil) as the sensing element. This particular balance section is designed to measure axial loads in the range from 0.1 to 6.0 pounds with an accuracy of $\pm$ 1 percent. This balance section is mentioned merely to serve as an example of the work in progress to improve the accuracy and extend the range of our static load balances.

Internal Strain-Gage Balances for Dynamic Measurements

35. Work is now in progress to develop balances which will measure dynamic loading on a model in the wind tunnel; specifically, this includes measuring (a) the Magnus forces acting on a spinning model, (b) measuring the damping-in-roll coefficients of a spinning model, and (c) measuring the damping-in-pitch coefficients of a pitching model.

36. A number of Magnus balances and attendant "drives" have been developed, some of which are capable of obtaining Magnus measurements at large angles of attack (40 to 90 degrees). These balances measure both normal and Magnus loads; therefore, they must be strong enough to withstand large normal loads and yet be "sensitive" enough to measure small Magnus loads. In most instances, the normal loads are of the order of 30 to 100 times the magnitude of the Magnus loads. A number of "drives" are in use which spin 1 1/4 inch to 3 inch diameter models at very high speeds. Electric motors are used to spin models up to 25,000 r.p.m.; air turbines are used to spin models up to 60,000 r.p.m.

37. The damping-in-roll balance can be used to obtain damping-in-roll measurements or to obtain the stabilized roll rate of a missile with fin cant. This balance is unlike other balances in that the strain gages rotate with the model. The strain-gage signals are transmitted from the model by means of "slip rings." At present, this balance can be used only at very small angles of attack and at spin rates up to 10,000 r.p.m.

38. The damping-in-pitch balance was designed to obtain damping coefficients by the damped oscillation technique. This balance is sting mounted and can be used only with blunt based bodies. The balance section is located inside the model. This balance was designed to allow the model to be located at various points along the axis of the balance; thus simulating different center of gravity locations with respect to the pivot flexure of the balance. The instantaneous angular diflection of the model is picked up by means of strain gages mounted at the flexure point (see reference c). Data can also be obtained by photographing a model mounted on ball bearings and supported by a wire rig. Both methods of obtaining data are in constant use.

39. With the dynamic balances enumerated above the versatility of the data obtained from wind-tunnel tests will be greatly enhanced thereby making the wind tunnel a more useful tool with which the aerodynamic designer can obtain the information he requires.
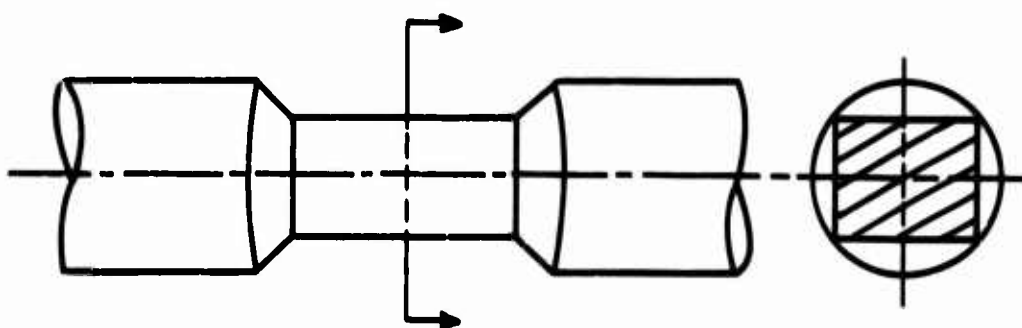
SUMMARY

40. This report has described the general design characteristics and the techniques employed in obtaining wind-tunnel data with internal strain-gage balances. The data reduction equations derived herein are general and are applicable to all cantilever balances of symmetrical cross-section which employ the two-moment method in obtaining normal force data.

References

(a) Gilbert, B. D. Automatic Data Processing System (ADAPS) for the Supersonic Wind Tunnels NavOrd Report 2613 (1953)

(b) DeMeritte, F. J., Gilbert, B. D., White, C. E. Contract Testing in the Naval Ordnance Laboratory Wind Tunnels Navord Report 3562 (1953)

(c) Shants, I. and Sparks, W. Damping-In-Pitch Measurements in the NOL 40 x 40 cm Aeroballistics Tunnels Navord Report 3859 (Unpublished)

**FIG. I TYPICAL PITCHING MOMENT AND YAWNING MOMENT
MEASURING SECTIONS**
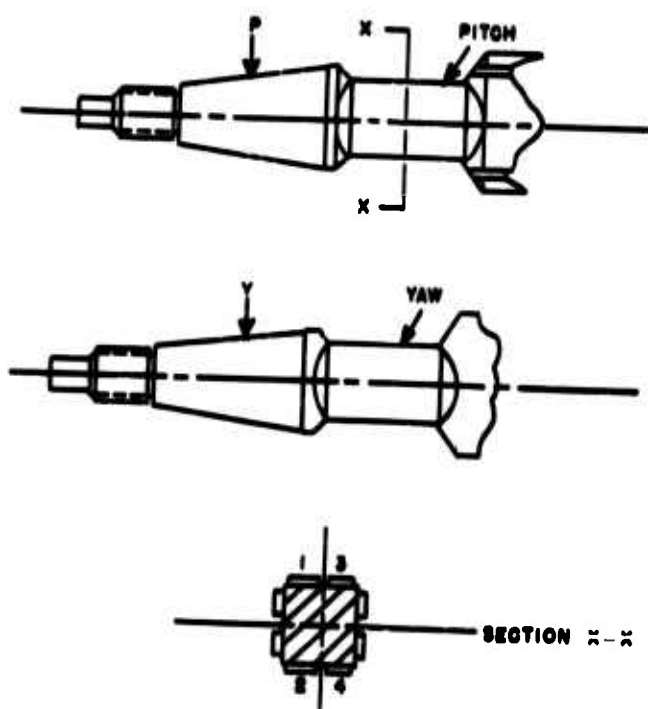
FIG. 2A PITCH AND YAW
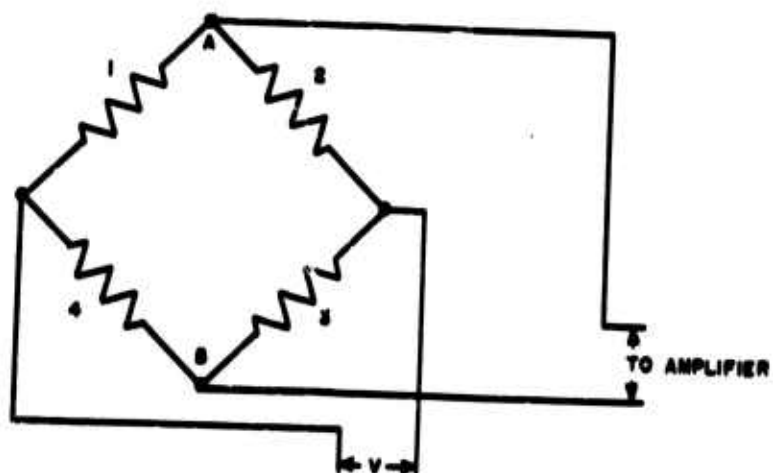
FIG. 2B

ROLL

FIG. 3A

SECTION Y-Y

FIG. 3B

TO AMPLIFIER

FIG. 3C

AXIAL

MEMBER FIXED TO AFT
STING SECTION

FIG. 4A

TO AMPLIFIER

FIG. 4B

TO
OTHER
COMPONENTS

TO
POWER

TO
AMPLIFIER
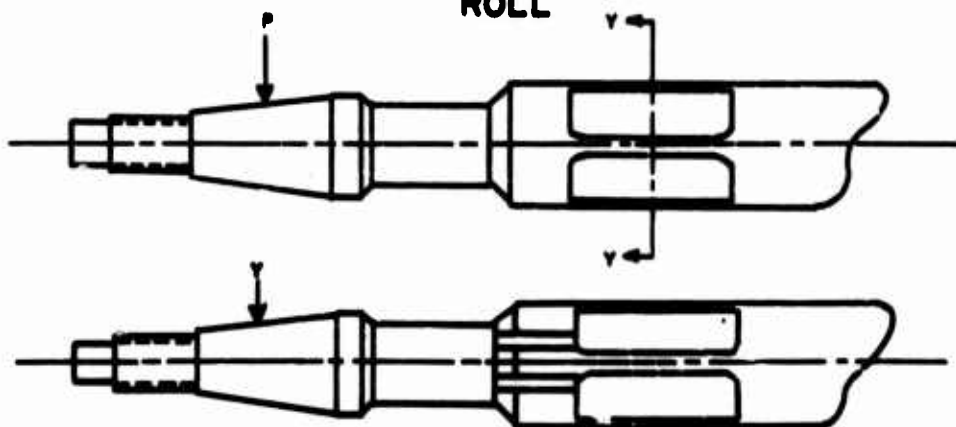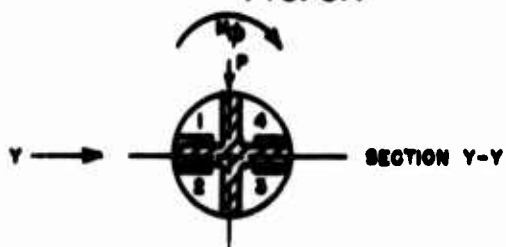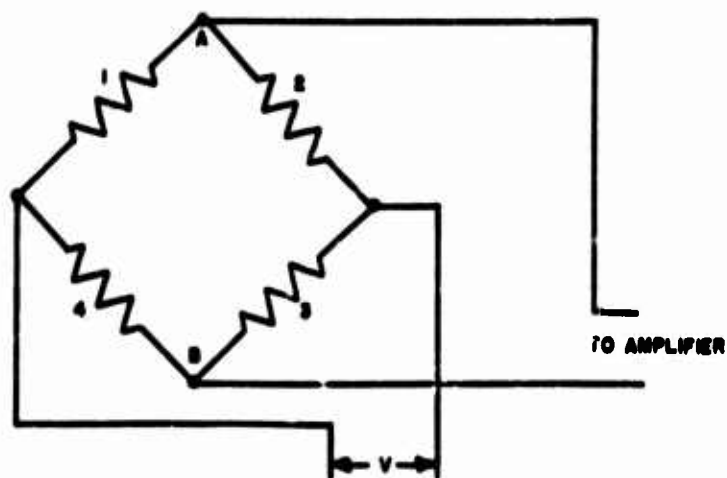
FIG. 4C

TYPICAL 6 – COMPONENT BALANCE

FIG. 5

FIG. 6A
INDICATION OF UNBALANCE BY MEANS
OF A SHUNTING POTENTIOMETER
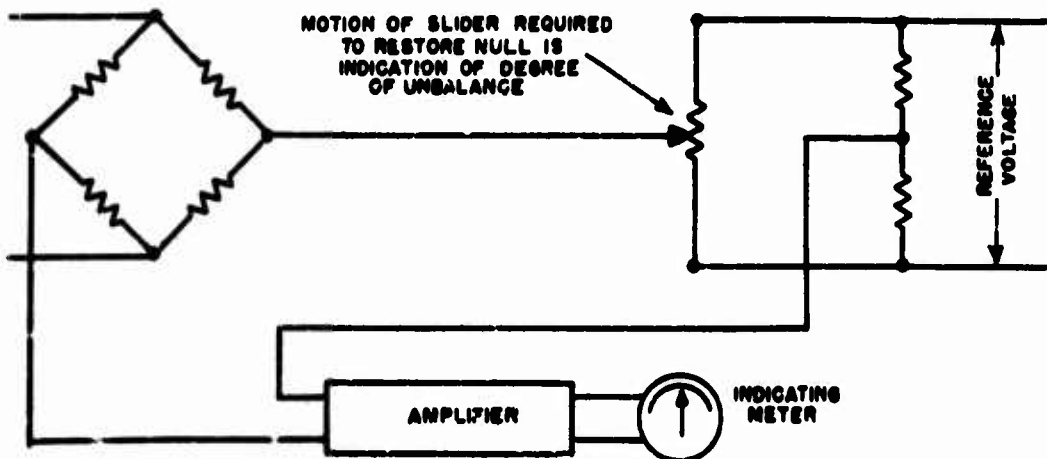
FIG. 6B
INDICATION OF UNBALANCE BY MEANS
OF A "BUCKING VOLTAGE" IN SERIES
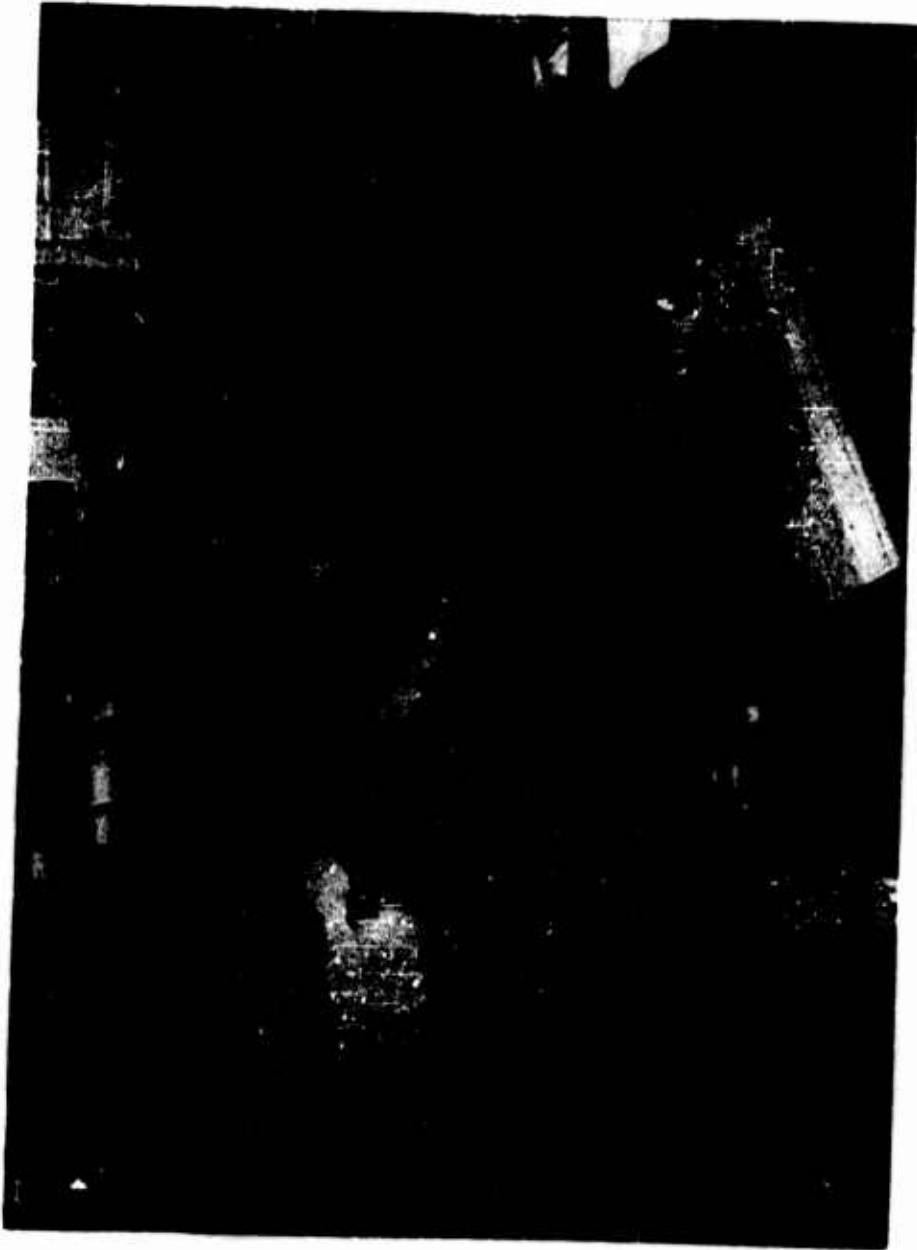
FIG 7 AUTOMATIC NULLING AND ATTENDANT IBM EQUIPMENT
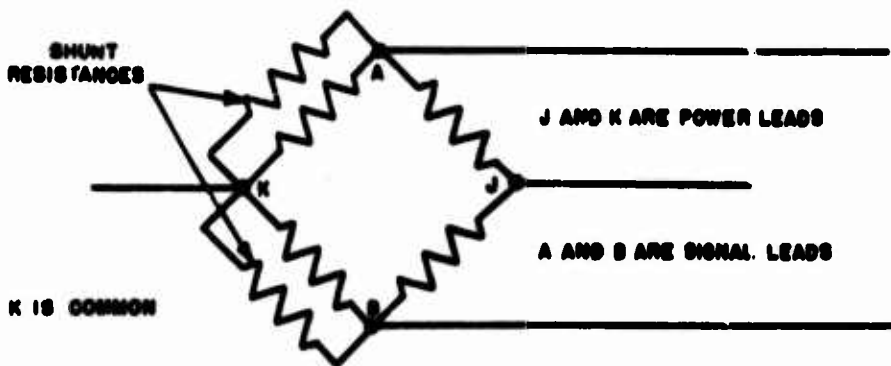
FIG. 8 DIAGRAMMATIC CIRCUIT LAYOUT FOR ELECTRICALLY
ALIGNED BRIDGE CIRCUIT

External Distribution List

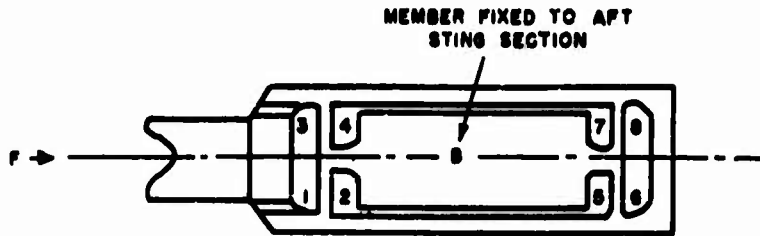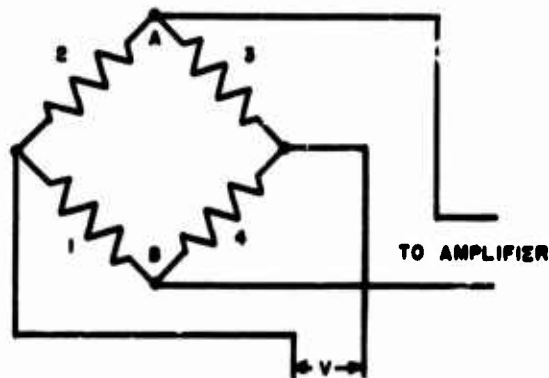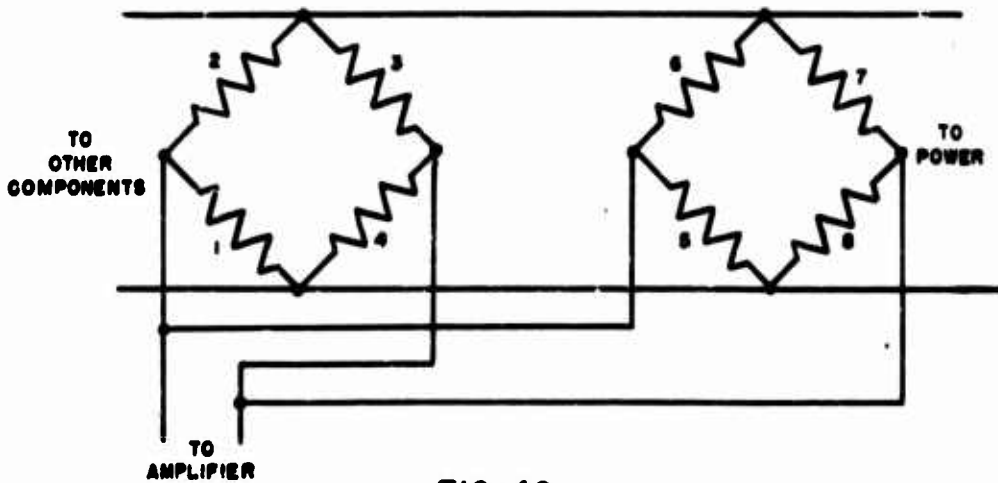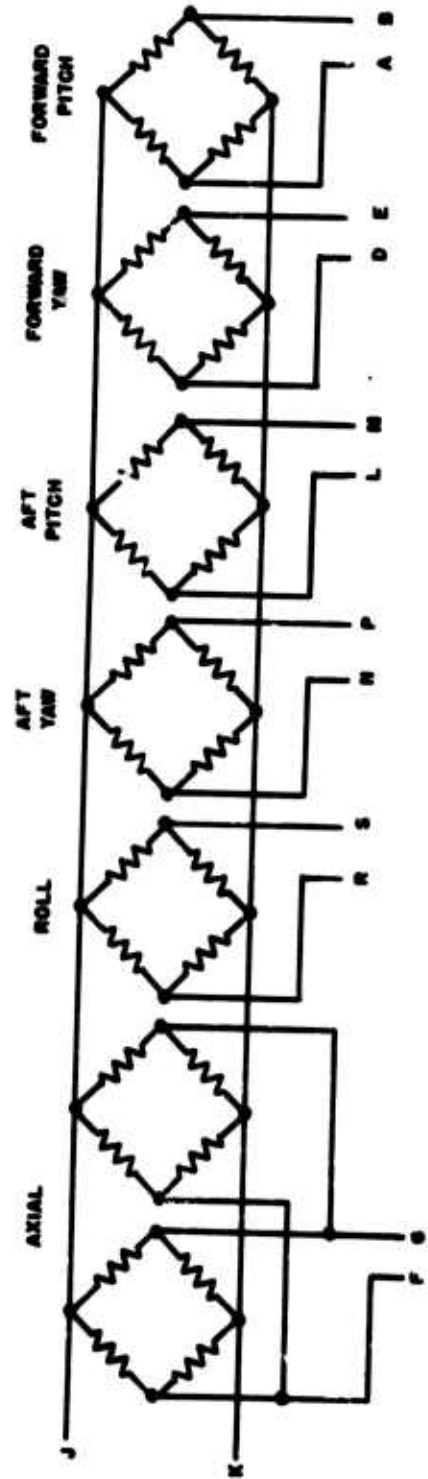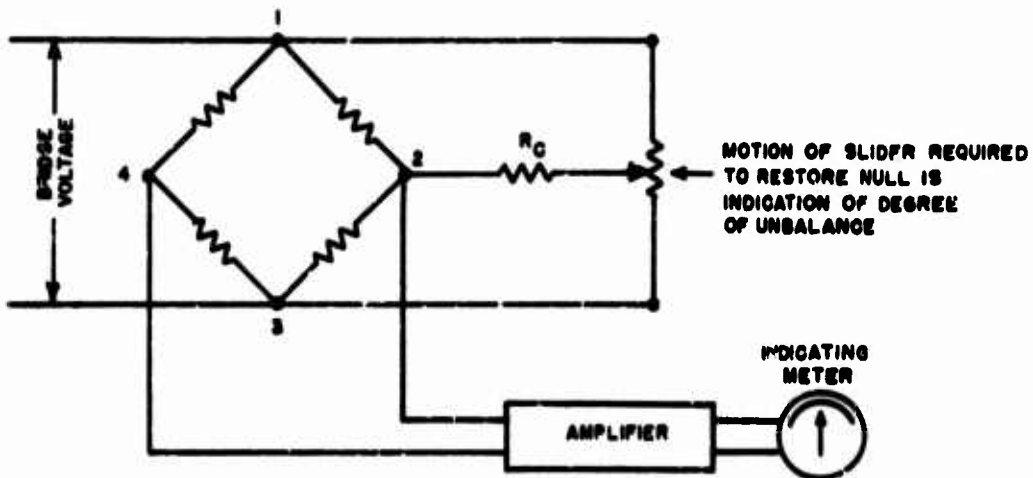|	No. of Copies
Chief, Bureau of Ordnance Department of the Navy Washington 25, D. C. Attn: Re3d Re9a	3 3
Washington Air Force Development Field Office Room 3016, Main Navy Building Washington 25, D.C. Attn: Major R. B. Robinson	1

Commanding General
Wright Air Development Center
Wright Patterson Air Force Base, Ohio
Attn: WCOWB
    WCOST
    WCS
    WCLS
    WCR
    WCOSI
	1
	1
	1
	1
	1
	1

U. S. Naval Ordnance Test Station Inyokern, China Lake, California Attn: W. R. Haseltine L. T. Jagiello	1 1
U. S. Naval Proving Ground Dahlgren, Virginia Attn: Dr. C. J. Cohen	1
Convair Corporation A Division of General Dynamics Fort Worth, Texas Attn: G. C. Grogan	1
Convair Corporation A Division of General Dynamics San Diego, California Attn: D. D. Bennett G. L. Shue	1 1
Chief, Bureau of Aeronautics Department of the Navy Washington 25, D.C. Attn: Aero and Hydro Branch	1
General Electric Company Building #1, Campbell Avenue Plant Schenectady, New York Attn: I. H. Edelfelt	1

No. Copies

Bell Aircraft Corporation
Niagara Falls, New York
Attn: P. Emmons   1

Redstone Arsenal
Huntsville, Alabama
Attn: R. J. Hay   1
     T. G. Reed   1

Boeing Airplane Company
Seattle, Washington
Attn: James Brinkmall   1

Aero Engineering Department
New York University
The Bronx, New York
Attn: F. K. Teichmann   1

ARO, Incorporated
Tullahoma, Tennessee
Attn: R. Mehlson   1
    K. Ross   1

Ballistics Research Laboratory
Aberdeen Proving Ground
Aberdeen, Maryland
Attn: E. R. Mhley   1

Southern California Cooperative Wind Tunnel
930 South Raymond Avenue
Pasadena 2, California
Attn: J. R. Smith   1

Cornell Aeronautical Laboratory, Inc.
4455 Genesee Street
Buffalo 21, New York
Attn: E. R. Bird   1

Aerodynamics Laboratory
U. S. Navy David Taylor Model Basin
Washington 7, D. C.
Attn: H. T. Jefferson   1

Jet Propulsion Laboratory
California Institute of Technology
4800 Oak Grove
Pasadena 3, California
Attn: E. M. Schurmeier   1

Temco Aircraft Corporation
P. O. Box 6191
Dallas 2, Texas
Attn: Library   1

No. Copies

Naval Supersonic Laboratory
Massachusetts Institute of Technology
560 Memorial Drive
Cambridge 39, Massachusetts
Attn: D. E. Ross   1

Aerodynamic Test Division
University of S. California Engineering Center
U. S. Naval Air Missile Test Center
Pt. Mugu, California
Attn: J. M. Carrington   1

North American Aviation, Inc.
International Airport
Los Angeles 45, California
Attn: F. W. Furry   1

Ordnance Aerophysics Laboratory
Convair Corporation
A Division of General Dynamics
Daingerfield, Texas
Attn: R. J. Vollum   1

Research Department
United Aircraft Corporation
400 Main Street
East Hartford 8, Connecticut
Attn: I. Twomey   1

Supersonic Wind Tunnel
Engineering Research Institute
University of Michigan
Ann Arbor, Michigan
Attn: H. P. Liepmann   1

University of Minnesota
Department of Aeronautical Engineering
Rosemount Aeronautical Laboratory
Minneapolis 14, Minnesota
Attn: L. J. Rasmussen   1

Commander
Wright Air Development Center
Wright-Patterson Air Force Base, Ohio
Attn: A. B. Buckley   1

Applied Physics Laboratory
The Johns Hopkins University
8621 Georgia Avenue
Silver Spring, Maryland
Attn: Dr. F. K. Hill   1
      Dr. C. N. Warfield   1
      A. E. Bonney   1
      L. L. Cronvich   1
      J. Walker   1

No. Copies

Department of Aeronautical Engineering
The Ohio State University
Columbus 10, Ohio
Attn: Dr. C. L. Von Eschen   1

Gas Dynamics Laboratory
Princeton University
Princeton, New Jersey
Attn: S. M. Bogdonoff   1

Boeing Airplane Company
Seattle Division
Seattle, Washington
Attn: O. S. Schairer   1

Ralph M. Parsons Company
Frederick, Maryland
Attn: K. R. Tinlin   1

Picatinny Arsenal
Dover, New Jersey
Attn: A. A. Novack   1

Chamberlin Corporation
Waterloo, Iowa
Attn: I. Herman   1

General Electric Company
Cincinnati, Ohio
Attn: M. Fousher   1

Norwegian Defense Research Establishment
Lillehagen, Norway
Attn: Didrik C. Sveding   1

ASTIA, Dayton Ohio   5